

Alma Mater Studiorum Università di Bologna  
Archivio istituzionale della ricerca

Supported Gold Nanoparticles for Alcohols Oxidation in Continuous-Flow Heterogeneous Systems

This is the final peer-reviewed author's accepted manuscript (postprint) of the following publication:

*Published Version:*

Supported Gold Nanoparticles for Alcohols Oxidation in Continuous-Flow Heterogeneous Systems / Ballarin, Barbara; Barreca, Davide; Boanini, Elisa; Cassani, Maria Cristina; Dambruoso, Paolo; Massi, Alessandro; Mignani, Adriana; Nanni, Daniele; Parise, Chiara; Zaghi, Anna. - In: ACS SUSTAINABLE CHEMISTRY & ENGINEERING. - ISSN 2168-0485. - STAMPA. - 5:6(2017), pp. 4746-4756. [10.1021/acssuschemeng.7b00133]

*Availability:*

This version is available at: <https://hdl.handle.net/11585/602436> since: 2017-06-26

*Published:*

DOI: <http://doi.org/10.1021/acssuschemeng.7b00133>

*Terms of use:*

Some rights reserved. The terms and conditions for the reuse of this version of the manuscript are specified in the publishing policy. For all terms of use and more information see the publisher's website.

This item was downloaded from IRIS Università di Bologna (<https://cris.unibo.it/>).  
When citing, please refer to the published version.

(Article begins on next page)

This is the final peer-reviewed accepted manuscript of:

*“Supported gold nanoparticles for alcohols oxidation in continuous-flow heterogeneous systems”*,  
B. Ballarin, D. Barreca, E. Boanini, M.C. Cassani, P. Dambrosio, A. Massi, A. Mignani, D. Nanni, C.  
Parise, A. Zaghi, *ACS Sustain. Chem. Eng.*, **2017**, 5, 4746-4756.

The final published version is available online at: DOI:  
[10.1021/acssuschemeng.7b00133](https://doi.org/10.1021/acssuschemeng.7b00133)

Rights / License:

The terms and conditions for the reuse of this version of the manuscript are specified in the publishing policy. For all terms of use and more information see the publisher's website.

This item was downloaded from IRIS Università di Bologna (<https://cris.unibo.it/>)

**When citing, please refer to the published version.**

# Supported Gold Nanoparticles for Alcohols Oxidation in Continuous-Flow Heterogeneous Systems

*Barbara Ballarin,<sup>a</sup> Davide Barreca,<sup>b</sup> Elisa Boanini,<sup>c</sup> Maria Cristina*

*Cassani,<sup>a\*</sup> Paolo Dambruoso,<sup>d</sup> Alessandro Massi,<sup>e</sup> Adriana Mignani,<sup>a</sup>*

*Daniele Nanni,<sup>a\*</sup> Chiara Parise,<sup>a</sup> and Anna Zaghi<sup>e</sup>*

*<sup>a</sup>Dipartimento di Chimica Industriale "Toso Montanari", Università di Bologna, Via Risorgimento 4, I-40136, Bologna, Italy; <sup>b</sup>CNR-ICMATE and INSTM, Department of Chemistry, Padova University, Via F. Marzolo, 1, I-35131, Padova, Italy; <sup>c</sup>Dipartimento di Chimica "Giacomo Ciamician", Università di Bologna, Via Selmi 2, I-40126, Bologna, Italy; <sup>d</sup>Istituto per la Sintesi Organica e la Fotoreattività, Consiglio Nazionale delle Ricerche, Via P. Gobetti, 101, I-40129, Bologna, Italy; <sup>e</sup>Dipartimento di Scienze Chimiche e Farmaceutiche, Università di Ferrara, Via Fossato di Mortara 17, I-44121, Ferrara, Italy.*

\*To whom correspondence should be addressed. E-mail: maria.cassani@unibo.it (M.C.C.), fax: +39 051 2093690; tel: +39 051 2093700; daniele.nanni@unibo.it (D.N.), fax: +39 051 2093654; tel: +39 051 2093623.

## Abstract

Gold nanoparticles ( $\text{Au}_{\text{NPs}}$ ) were anchored on alkynyl carbamate-functionalized support materials having the suitable features for application as catalysts in continuous-flow packed bed reactors. The functionalization step was carried out by grafting with the di-functional organosilane [3-(2-propynylcarbamate)propyl]triethoxysilane (PPTEOS) three commercial micrometer-sized oxide supports, i.e. silica, alumina, and titania. The alkynyl-carbamate moieties were capable to straightforwardly reduce the gold precursor  $\text{HAuCl}_4$  yielding the supported  $\text{Au}_{\text{NPs}}$  systems **Au/SiO<sub>2</sub>@Yne**, **Au/Al<sub>2</sub>O<sub>3</sub>@Yne**, and **Au/TiO<sub>2</sub>@Yne**. A comparison among the three materials revealed that silica allowed the highest organic functionalization (12 wt%) as well as the highest gold loading (3.7 wt%). Moreover, TEM investigation showed only for **Au/SiO<sub>2</sub>@Yne** the presence of homogeneously distributed, spherically shaped  $\text{Au}_{\text{NPs}}$  (av. diameter 15 nm). **Au/SiO<sub>2</sub>@Yne** is an efficient catalyst, both in batch and flow conditions, in the oxidation of a large variety of alcohols, using  $\text{H}_2\text{O}_2$  as oxidizing agent, at a temperature of 90 °C. Furthermore, under flow conditions, the catalyst worked for over 50 h without any significant decrease in the catalytic activity. The catalytic activity of the three catalysts was evaluated and compared in the oxidation of 1-phenylethanol as a model substrate. We found that the flow approach plays a strategic role in preserving the physical and chemical integrity of the solid catalysts during its use, with remarkable consequences for the reaction conversion (from 2% in batch to 80 % in flow) in the case of **Au/TiO<sub>2</sub>@Yne**.

**Keywords:** gold nanoparticles, alkynyl carbamate functionalized oxide supports, heterogeneous catalysis, alcohol oxidation, continuous-flow packed bed reactors.

## Introduction

Alcohol oxidation is one of the most important transformations in industrial organic chemistry and a challenging one in terms of green chemistry.<sup>1,2</sup> Traditional methods involve the use of toxic, expensive stoichiometric metal oxidants and harmful organic solvents, and they often require vigorous reaction conditions.<sup>3,4</sup> On the other hand, gold nanoparticles (Au<sub>NPs</sub>), especially supported gold nanoparticles, can successfully oxidize alcohols in aqueous media by means of air, O<sub>2</sub>, or H<sub>2</sub>O<sub>2</sub>.<sup>5-23</sup>

Flow chemistry is another emerging topic of current widespread interest that has been recognized by the Green Chemistry Institute (GCI) as a key area for research activities, with the aim of developing sustainable manufacturing.<sup>24-27</sup> The main advantages of a flow reactor are: i) the use of small volumes, which allows a perfect control of exothermic processes by preventing accumulation of intermediates; ii) the fast heating and mass transfer, which provide an instantaneous and homogenous mixing; iii) the very efficient thermal management, which makes the flow systems really safe by preventing thermal runaways and hot spots; iv) the high pressure stability, enabling to run reactions at lower temperature; v) the possibility of reducing the quantity of solvents and even to carry out solvent-free reactions. In the flow nanocatalysis approach the advantages of both nanocatalysis and flow chemistry are exploited and boosted.<sup>28-30</sup>

In our previous works we have presented the preparation, without any need of additional reducing and/or stabilizing agents, of a variety of stable silica-supported Au<sub>NPs</sub> by using different functionalized-silica supports and a chloroauric acid (HAuCl<sub>4</sub>) aqueous solution as the only reactants.<sup>31-34</sup> We started using commercial polyethyleneimine-functionalized silica beads<sup>30</sup> and we went on preparing silica nanoparticles with alkynyl carbamate moieties synthesized by co-condensation of the di-functional organosilane [3-(2-propynylcarbamate)propyl]triethoxysilane (PPTEOS) with tetraethoxysilane (TEOS) in alkaline medium. By this method, spherical and monodispersed functionalized silica nanoparticles with a porous structure and an average size distribution of 45 nm could be obtained. The synergistic effect of the carbamate and alkynyl

functionalities present on the silica surface was exploited for the smooth reduction of  $\text{HAuCl}_4$  and successive stabilization of the resulting silica-supported  $\text{Au}_{\text{NPs}}$ .<sup>31,32</sup> PPTEOS, through its derivatization by radical thiol-yne chemistry, was subsequently used to fabricate a novel amino-sulfide branched silica support suitable for the preparation of analogous  $\text{Au}_{\text{NPs}}$ -based catalytic systems.<sup>34</sup>

In the present work we have anchored  $\text{Au}_{\text{NPs}}$  on some alkyne-modified support materials having the right features for the application as catalysts in continuous-flow packed bed reactors.<sup>23,35,36</sup> Indeed the functionalization step was carried out by grafting with PPTEOS three commercial micrometer-sized oxide supports (abbreviated **OS**), *i.e.* silica, alumina, and titania. We first investigated the catalytic activity of **Au/SiO<sub>2</sub>@Yne** in the oxidation of primary and secondary alcohols, then the oxidation of 1-phenylethanol was taken as a model reaction to examine and compare the catalytic activities of **Au/SiO<sub>2</sub>@Yne**, **Au/Al<sub>2</sub>O<sub>3</sub>@Yne**, and **Au/TiO<sub>2</sub>@Yne** (hereafter generically named as **Au/OS@Yne**). The catalytic tests were carried out both in batch and under continuous-flow conditions at a temperature of 90°C using, depending on the substrate, water or a  $\text{H}_2\text{O}/\text{BuOH}$  (6:4 v/v) mixture as the reaction medium and  $\text{H}_2\text{O}_2$  as the oxidizing agent.

## Experimental Section

**Materials.** Triethylamine (TEA, 99%), hydrogen peroxide ( $\text{H}_2\text{O}_2$ , 35 wt% in  $\text{H}_2\text{O}$ ), sodium hydroxide (NaOH), benzyl alcohol, 4-nitrobenzyl alcohol, 4-methylbenzyl alcohol, 4-methoxybenzyl alcohol, 1-octanol, 2-octanol, 1-phenylethanol, diphenylmethanol, cyclohexanol, 1-(4-chlorophenyl)ethanol, 1-(4-fluorophenyl)ethanol, 1-(p-tolyl)ethanol, 4-methoxy- $\alpha$ -methylbenzyl alcohol,  $\alpha$ -methyl-2-naphthalenemethanol, 1,7-heptanediol, ethanol (99%), dichloromethane (DCM, 99%), tert-butanol ( $\text{tBuOH}$ , 99%), ethyl acetate (EtOAc), and deuterated chloroform ( $\text{CDCl}_3$ ) were of analytical grade and were used as purchased from Sigma-Aldrich. Toluene was dried over Na/K alloy and distilled under nitrogen prior to use. Ultrapure water purified with the Milli-Q plus system (Millipore Co, resistivity over 18  $\text{M}\Omega$  cm) was used in all cases.  $\text{HAuCl}_4 \cdot 3\text{H}_2\text{O}$  was prepared

according to a literature procedure;<sup>37</sup> [3-(2-propynylcarbamate)propyl]triethoxysilane (PPTEOS) was prepared as previously reported.<sup>31</sup> Commercial silica gel for column chromatography (particle size 70-230 mesh, pore volume c.a. 0.8 cm<sup>3</sup>/g, surface area 550 m<sup>2</sup>/g, Sigma-Aldrich) and aluminum oxide 90 active neutral (particle size 70-230 mesh, pore volume ca. 0.27 cm<sup>3</sup>/g, surface area ca. 120 m<sup>2</sup>/g, Merck) were dried prior to use by heating at 180 °C in a quartz tube under a slow stream of dry nitrogen and then stored under nitrogen.<sup>38</sup> Titanium oxide (Cristal ACTIV DT-51, 100% anatase, surface area ca. 90 m<sup>2</sup>/g), purchased from Cristal (www.cristal.com), was first pelletized into a 30 mm diameter disk. The pellets were subsequently gently crumbled and sieved, first on a 60 mesh stainless steel sieve (Filtro Vibracions S.L.) and then on a 80 mesh sieve. Only the powder that remained on the 80 mesh sieve was used in the grafting process. The commercial Au/TiO<sub>2</sub> catalyst AUROLite™ (Gold 1 wt% on titanium dioxide extrudates purchased from Strem) was mildly ground in an agate mortar and then passed on a 80 mesh stainless steel sieve. Only the material with particle size higher than 80 mesh was employed in the catalytic tests.

**Preparation of OS@Yne.** The grafting of the PPTEOS on the silica surface was performed under N<sub>2</sub> atmosphere at 60 °C. A 100 mL three-necked dry round-bottomed flask was charged with SiO<sub>2</sub> (4.73 g), TEA (98 μL, 0.70 mmol) and toluene (17 mL). An excess of PPTEOS (2.29 g, 7.58 mmol), previously dissolved in toluene (12 mL), was added to the vigorously stirred mixture. The reaction mixture was stirred for 23 h at 60 °C, then the temperature was raised to 100 °C and the nitrogen flow was increased in order to remove ethanol, formed as a co-product, and to reduce the mixture volume. The obtained **SiO<sub>2</sub>@Yne** was isolated by centrifugation (5600 rpm, 15 min) and re-dispersed in EtOH. The re-dispersion/centrifugation procedure was repeated three times while the excess of PPTEOS was recovered from the supernatant solution. The samples were dried in oven at 50 °C for 3 h and kept under a nitrogen stream to remove the residual solvent, finally yielding a white powder.

The grafting of aluminum oxide (**Al<sub>2</sub>O<sub>3</sub>@Yne**) was performed following the same procedure. A solution of PPTEOS (2.67 g, 8.84 mmol) in 18 mL of toluene was added to a suspension of Al<sub>2</sub>O<sub>3</sub> (6.99 g) and TEA (115 μL, 0.83 mmol) in 20 mL of toluene.

The functionalization of titanium oxide (60-80 mesh, prepared as described in the previous paragraph) was carried out as follows. A dry round-bottomed flask kept under a nitrogen atmosphere was charged with TiO<sub>2</sub> (2.05 g), TEA (42 μL, 0.30 mmol), and toluene (10 mL), then a solution of PPTEOS (0.99 g, 3.29 mmol) in toluene (5 mL) was added. The flask was then connected to a rotary evaporator, heated at 60 °C, and left under stirring at 60 rpm for 9 h. At the end of the reaction the obtained **TiO<sub>2</sub>@Yne** was isolated by centrifugation, washed three times with ethanol, and dried under a nitrogen stream.

#### **Preparation of Au/OS@Yne.**

**Au/SiO<sub>2</sub>@Yne.** The preparation of **Au/SiO<sub>2</sub>@Yne** was carried out in a 500 mL three-necked dry round-bottomed flask under a N<sub>2</sub> atmosphere. The flask was first charged with 1.0 g of **SiO<sub>2</sub>@Yne** and 100 mL of H<sub>2</sub>O and the suspension was heated to 90 °C. After reaching the desired temperature, HAuCl<sub>4</sub>·3H<sub>2</sub>O (0.0980 g, 0.25 mmol), previously dissolved in 150 mL of H<sub>2</sub>O, was added in order to have a 1.00 mM of HAuCl<sub>4</sub>·3H<sub>2</sub>O as the final concentration; the reaction mixture was left under stirring for 1 h.

**Au/Al<sub>2</sub>O<sub>3</sub>@Yne.** The synthesis was performed following the same procedure of **Au/SiO<sub>2</sub>@Yne**, starting with a suspension of 1.033 g of **Al<sub>2</sub>O<sub>3</sub>@Yne** in 100 mL of H<sub>2</sub>O, and then adding a solution of 0.0994 g of HAuCl<sub>4</sub> previously dissolved in 150 mL of H<sub>2</sub>O.

**Au/TiO<sub>2</sub>@Yne.** This synthesis was carried out in a rotary evaporator, without the use of a magnetic stirrer. A two-necked flask was charged with 0.972 g of **TiO<sub>2</sub>@Yne** and 100 mL of H<sub>2</sub>O and heated to 90 °C. When the desired temperature was reached, a solution of 0.0995 g of HAuCl<sub>4</sub> dissolved in 150 mL of H<sub>2</sub>O was rapidly added and the reaction mixture was left under stirring at 60 rpm for 1 h.

In all the three procedures, after the addition of the gold precursor a rapid change in the colour of the solution from pale-yellow to red-purple was observed. At the end of the reaction the



obtained solid material was separated from the supernatant solution by centrifugation (5600 rpm, 15 min) and re-dispersed twice in water and twice in EtOH, then it was dried under a nitrogen flow. Successively, **Au/TiO<sub>2</sub>@Yne** was passed again on a 80 mesh stainless steel sieve (Filtro Vibraciones S.L.) and only the powder with particle size higher than 80 mesh (ca. 50%) was used in the catalytic tests.

Detailed information regarding instruments and methods employed for material characterization (TGA, TEM, ATR-FTIR, AAS, NMR, GC) are reported in the Supplementary Information. Solid State NMR spectra (SS NMR) were recorded using adamantane as reference on an Agilent NMR system, consisting of a 54-mm bore, 11.7 Tesla Premium Shielded superconducting magnet, a DD2 Performa IV NMR console equipped with 100 W highband and 300 W lowband amplifiers, and a NB Agilent 3.2 mm T3 MAS HXY Solid Probe 500 MHz.

X-ray photoelectron spectroscopy (XPS) analyses were conducted on a Perkin-Elmer  $\Phi$  5600ci spectrometer using a standard AlK $\alpha$  excitation source ( $h\nu = 1486.6$  eV), at a working pressure  $< 10^{-8}$  mbar. The reported binding energies (BEs; uncertainty =  $\pm 0.1$  eV) were corrected for charging effects by assigning a BE of 284.8 eV to the C1s line of adventitious carbon.<sup>39,40</sup> After a Shirley-type background subtraction,<sup>41</sup> atomic percentages (at. %) were calculated by signal integration using sensitivity factors supplied by Perkin-Elmer. Peak fitting was performed adopting Gaussian-Lorentzian peak shapes by means of the XPS Peak software (version 4.1; <http://xpspeak.software.informer.com/4.1/>).

The system used for continuous-flow reactions was composed of an HPLC pump (Agilent 1100 micro series), an in-line pressure transducer, a thermostated microreactor holder (Peltier unit), a system to collect fractions, and a data acquisition system (Agilent ChemStation). The units were connected by peek tubing (internal diameter 0.01 inch from Upchurch Scientific). The system hold-up volume was smaller than 80  $\mu$ L. The temperature was controlled by inserting a thermometer inside the Peltier unit (temperature measurement error:  $\pm 0.5$  °C).

## Catalytic tests.

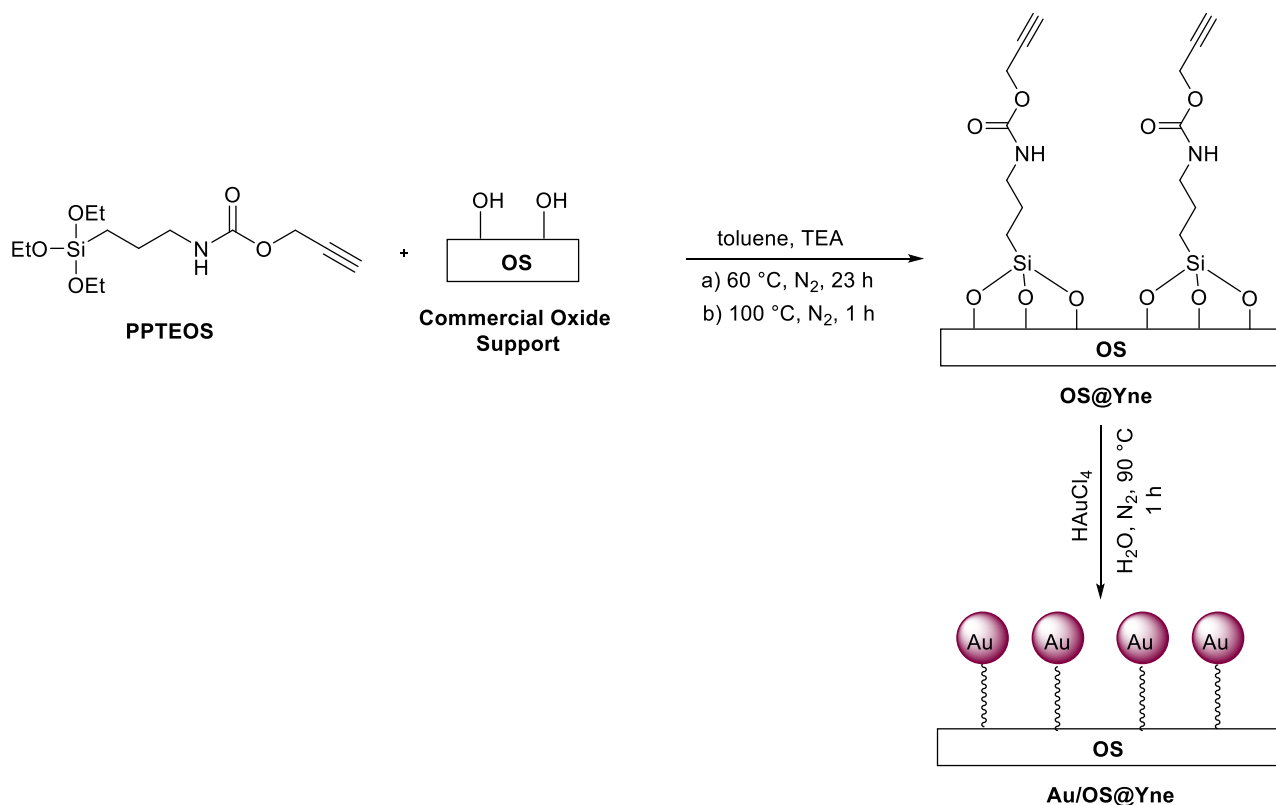
*Batch experiments.* In a typical procedure a 0.1 M solution of the starting alcohol in the appropriate solvent medium and 1 % mol Au catalyst were charged in a flask and stirred for a few minutes at 90 °C, then 2.5 molar equivalents of H<sub>2</sub>O<sub>2</sub> were added. At the end of the reaction the solid catalyst was separated from the mixture by centrifugation and washed once with water and once with DCM, then the reactants and the products were recovered from the aqueous phase by extraction with DCM and analyzed by <sup>1</sup>H-NMR to evaluate the yield of the carbonyl compounds. A comparison between the conversion determined by <sup>1</sup>H-NMR analysis and GC analysis was also carried out in the case of the benzyl alcohol substrate. For the GC analysis the aqueous phase isolated at the end of the reaction was directly analyzed. Calibration lines for benzyl alcohol, benzoic acid, and benzaldehyde were obtained after injection of four aqueous solutions at a known concentration, employing 1,7-heptanediol as internal standard. For recycling tests, the catalyst was recovered by centrifugation and washed first with H<sub>2</sub>O and then three times with ethyl acetate before being reused in the next cycle. With the TiO<sub>2</sub>-supported catalyst vertical agitation was performed with the FirstMate™ synthesizer, Argonaut Technology.

*Continuous-Flow experiments.* The microreactors used for the continuous-flow experiments were prepared by gravity packing a 10 cm long column (internal diameter 2.1 mm, Figure S7) with **Au/OS@Yne** (300 ÷ 400 mg depending on the Au wt. % content). In a typical procedure, the continuous-flow system was fed with a 0.1 M solution of the alcohol at 30 °C and operated at a flow rate of 0.1 mL min<sup>-1</sup>, with the packed microreactor heated to 90 °C. Hydrogen peroxide was added to the reagent mixture just before running. The eluate was collected in several fractions and analyzed by <sup>1</sup>H-NMR after extractions with DCM.

## Results and Discussion

**Preparation and characterization of Au/OS@Yne.** The first step was the modification of the support with the alkynyl carbamate-terminated organosilane PPTEOS. The condensation reaction

between the organosilane and the hydroxyl groups present on the surface was carried out in toluene, under nitrogen, in the presence of TEA (Scheme 1).



**Scheme 1.** Preparation of **Au/OS@Yne** [OS = SiO<sub>2</sub> and Al<sub>2</sub>O<sub>3</sub> (70-230 mesh), TiO<sub>2</sub> (60-80 mesh)].

In the second step the preparation of **Au/OS@Yne** was carried out in an aqueous medium at 90 °C under nitrogen. The formation of the Au<sub>NPs</sub> was obtained by simply adding an aqueous solution of H<sub>2</sub>AuCl<sub>4</sub> to a dispersion of **OS@Yne**. Within the first minutes of the reaction the colour rapidly changed from pale-yellow to violet. After 1 h, the suspension was centrifugated to remove the supernatant solution, which was colourless, suggesting the absence of free Au<sub>NPs</sub>. The solid **Au/OS@Yne** was washed by means of centrifugation/re-dispersion in water and EtOH, and finally dried to obtain a purple powder.<sup>42,43</sup>

The **Au/OS@Yne** samples were characterized by TGA analyses, AAS, ATR-FTIR, XPS spectroscopy and TEM microscopy; the most important data are summarized in Table 1.

**Table 1.** TGA, AAS, and TEM data for **Au/OS@Yne**

Sample	Yne (wt %) <sup>a</sup>	Au (wt%) <sup>b</sup>	Au <sub>NPs</sub> d <sub>TEM</sub> (nm)
<b>Au/SiO<sub>2</sub>@Yne</b>	12 ± 1	3.7 ± 0.1	15 ± 4
<b>Au/Al<sub>2</sub>O<sub>3</sub>@Yne</b>	6 ± 1	2.0 ± 0.1	18 ± 7
<b>Au/TiO<sub>2</sub>@Yne</b>	2 ± 1	1.7 ± 0.1	large distribution

<sup>a</sup>weight loss by TGA; <sup>b</sup>determined by AAS.

The TGA analyses, used to evaluate the efficiency of the grafting process, showed for **Au/SiO<sub>2</sub>@Yne** (Figure S1a) three regions of mass loss associated to evaporation of adsorbed water and ethanol (30 – 150 °C), degradation of organic material (150 – 500 °C), and dehydration of SiOH groups (500 – 705 °C). The weight loss of the organic material was 12 wt %, in keeping with the expected organic moieties incorporation. Analogue thermograms were obtained from the analysis of **Au/Al<sub>2</sub>O<sub>3</sub>@Yne** (Figure S1b) and **Au/TiO<sub>2</sub>@Yne** (Figure S1c) samples, with a mass loss in the region of organic material degradation of 6 wt% and 2 wt%, respectively.

The exact content of gold in the catalyst was determined by AAS after each synthesis. The results of the AAS analyses indicated that the average value of gold loading is related to the degree of functionalization of the starting support. The silica-supported catalyst showed the highest loading of gold (average value 3.7 wt %), while in the case of alumina and titania lower loadings were found (2.0 wt % and 1.7 wt % respectively).

The morphology of **Au/OS@Yne** samples was investigated by TEM microscopy. The gold nanoparticles presented a spherical shape and were found to be attached on the support surface. **Au/SiO<sub>2</sub>@Yne** showed quite a uniform distribution of Au<sub>NPs</sub> with an average diameter of 15 ± 4 nm (Figure 1), whereas in the case of **Au/Al<sub>2</sub>O<sub>3</sub>@Yne** the nanoparticles seemed to form more aggregates and were on average larger (18 ± 7 nm) compared to the silica-supported catalyst

(Figure S2a). The TEM images of **Au/TiO<sub>2</sub>@Yne** presented a more random size distribution: the most part of particles shows a diameter ranging from 10 to 20 nm, but some very large particles (up to 70 nm) were observed (Figure S2b).

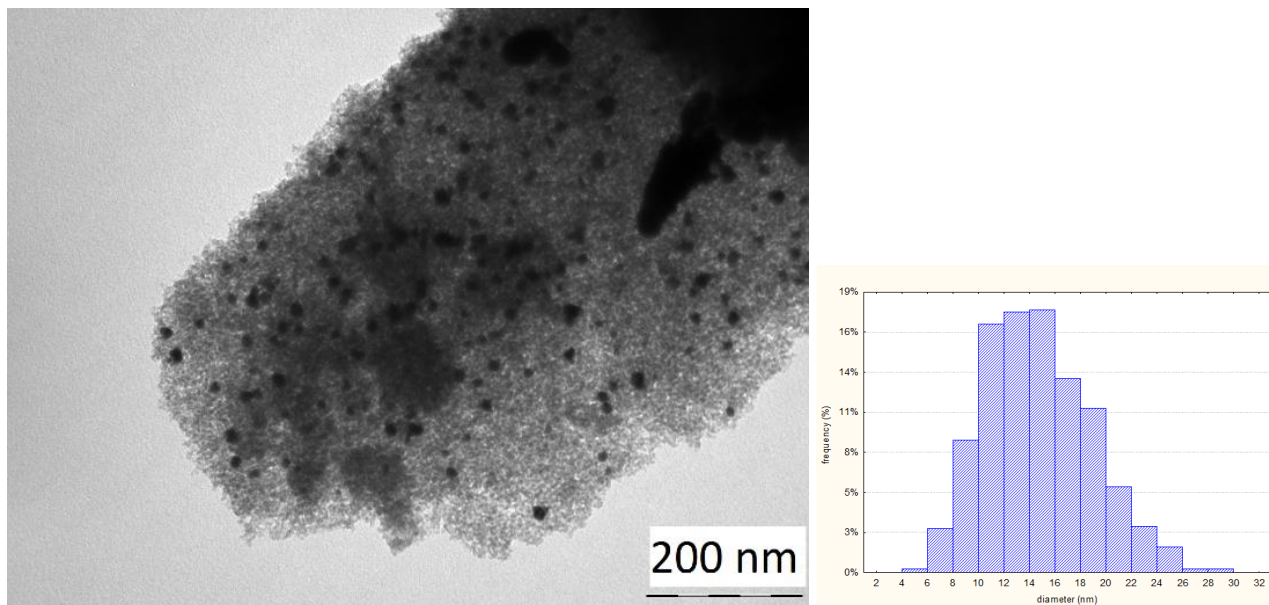


**Figure 1.** TEM image and particles size distribution of **Au/SiO<sub>2</sub>@Yne** ( $15 \pm 4$  nm).

The ATR-FTIR spectra of **Au/OS@Yne** were also recorded and in all cases the presence of the carbamate moiety was evidenced by the appearance of two bands at ca. 1700 and 1530  $\text{cm}^{-1}$ , associated to the C=O stretching and the N-H bending vibrations, respectively (Figure S3).<sup>44</sup>

The surface functionalization and the corresponding chemical modification along the synthetic pathway were also monitored, in the case of SiO<sub>2</sub>-immobilized Au<sub>NPs</sub>, by observing <sup>13</sup>C by SS NMR (both directly and via Cross Polarization experiments). Figure 2 shows a comparison between the <sup>13</sup>C CP/MAS NMR spectra of the commercial silica support, the functionalized **SiO<sub>2</sub>@Yne** microspheres, and the corresponding **Au/SiO<sub>2</sub>@Yne**.

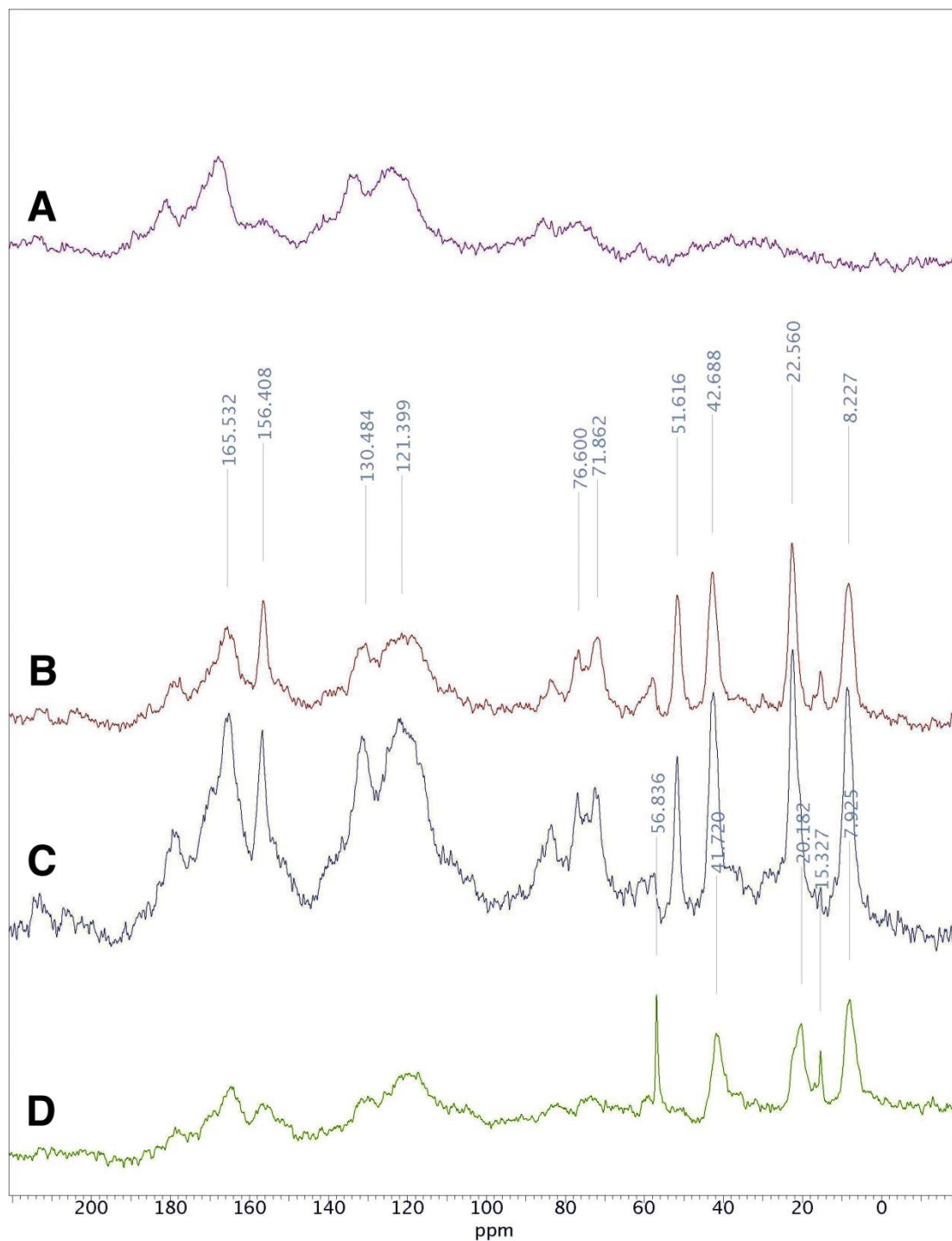


**Figure 2.**  $^{13}\text{C}$  CP/MAS NMR spectra recorded at 500 MHz. (A) the top spectrum corresponds to bare silica; (B)  $\text{SiO}_2@\text{Yne}$ ; (C)  $\text{Au}/\text{SiO}_2@\text{Yne}$  (Au = 3.7 wt%); (D)  $\text{Au}/\text{SiO}_2@\text{Yne}$  (Au = 13 wt%).

Apart from the very large signals (in the following spectrum regions: 70-90 ppm, 110-140 ppm, and 160-180 ppm) belonging to the commercial silica sample, the **SiO<sub>2</sub>@Yne** microspheres clearly evidenced all the relevant signals of the pendant: the aminopropylsilane linker (signals at 8.23, 22.56, and 42.69 ppm), the propargyl methylene (51.62 ppm), both alkyne carbons (76.60 and 83.45 ppm), and the carbamic carbonyl at 156.41 ppm.<sup>31</sup> At the same time, **Au/SiO<sub>2</sub>@Yne** (Figure 2C) containing 3.7 wt% of gold showed no relevant modification of the organic functionalization, as confirmed by the ATR-FTIR spectra. Therefore, in order to investigate the effect of the Au(III) to Au(0) reduction on the carbamate branch, a sample containing 13 wt% of gold was appositely prepared.<sup>45</sup> The corresponding CP/MAS NMR spectrum (Figure 2D) showed a significant decrease in the signals of the alkynyl and carbonyl carbons of the starting pendant but three quite strong signals (at 7.92, 20.18, and 41.72 ppm) ascribable again to an aminopropylsilane linker. This suggests that gold reduction led to some modification of the starting pendant likely involving the degradation of the propynylcarbamate moiety and likely resulting in an aminopropyl chain, responsible in turn for the eventual stabilization of the gold nanoparticles.<sup>30</sup>

The other strong two singlets at 15.33 and 56.84 ppm could be tentatively assigned to the methyl and methylene carbon atoms, respectively, of surface-bound ethoxy groups, deriving from condensation of the ethanol produced during the silica modification with the silica silanols, a process much more evident upon using larger amounts of chloroauric acid.<sup>46</sup>

The surface chemical composition of the target systems was analyzed by XPS. Wide-scan spectra (Figure 3a) displayed the presence of C, O, N and Au lines, as well as photopeaks related to the used oxide supports (silica, alumina, and titania; see also Figure S3), indicating that the organic functionalization was successfully obtained. This was further confirmed by the analysis of the main carbon peak. In fact, irrespective of the analyzed specimen, the C1s signal (Figure 3b) displayed a tailing towards the high BE side and was deconvoluted by means of three different bands, centered at mean BE values of 284.8 eV (**I**; 52-57% of the total C signal), 286.4 eV (**II**; 29-39% of the total C signal), and 289.2 eV (**III**; 9-14% of the total C signal). These components could be attributed to

C–C, C–H, and/or C–Si (**I**), C–N and/or C–O (**II**), and O–C=O (**III**) bonds, respectively.<sup>32,34,40</sup> More detailed calculations to estimate the different number of carbon atoms present on the species anchored to the substrate surface were avoided due to the fact that band **I** also contains contributions from adventitious carbon, whose occurrence is ubiquitous on the surface of air-exposed samples. Despite the contributions due to oxygen atoms in the ligand chains could not be resolved (see Supporting Information and Figure S3), being overlapped with the other more intense oxygen bands,<sup>32,34</sup> the successful anchoring of the target species to the substrates was confirmed by the analysis of the N1s photopeaks (Figure 3c), which resulted from the contributions of a main component (**IV**, BE = 399.5 eV, 36-50% of the total nitrogen), due to N in amino-groups<sup>40</sup> and an additional band (**V**, BE = 401.1 eV) related to NH-COO- groups.<sup>34</sup> This is in line with the presence of an aminopropylsilane linker evidenced by the <sup>13</sup>C CP/MAS NMR analysis (see above). Figure 3d displays the surface Au4f signals for the different specimens. Irrespective of the used substrate, no signals related to Au(I) and Au(III) species could be clearly identified, enabling thus to highlight the presence of pure Au aggregates, in agreement with previous studies. Typical surface at.% values for gold were 0.7 at.% for **Au/SiO<sub>2</sub>@Yne**<sup>32,34</sup> and **Au/TiO<sub>2</sub>@Yne**, and slightly higher for **Au/Al<sub>2</sub>O<sub>3</sub>@Yne** (0.8 at.%). This clearly shows that the presence of the carbamate group in the alkynyl moiety is essential to trigger reduction of Au(III) to Au(0) with respect to other alkyne/Au(III)-Au(I) complexes.<sup>47-49</sup>

Interestingly, the analysis of Au4f<sub>7/2</sub> BE evidenced a progressive downward shift upon going from SiO<sub>2</sub> to TiO<sub>2</sub>-supported specimens [BE(Au4f<sub>7/2</sub>) = 84.3, 84.0 and 83.4 eV for **Au/SiO<sub>2</sub>@Yne**, **Au/Al<sub>2</sub>O<sub>3</sub>@Yne** and **Au/TiO<sub>2</sub>@Yne** samples, respectively]. In general, gold nanoparticles can be either slightly positive or negative, depending on the adopted support, synthesis method and processing conditions.<sup>50,51</sup> For alumina and titania-supported samples, the peak position was in good agreement with previously reported data for homologous systems.<sup>52-54</sup> A comparison of the present BE data with the reference position for bulk metallic gold [BE(Au4f<sub>7/2</sub>) = 84.0 eV]<sup>39</sup> revealed a downward shift of Au peak position for **Au/TiO<sub>2</sub>@Yne**, suggesting the occurrence of



electron donation from titania support to the metal and the consequent formation of an electron-rich ( $\text{Au}^{\delta-}$ ) phase in this case.<sup>54-56</sup> In a different way, the BE increase with respect to bulk Au observed for **Au/SiO<sub>2</sub>@Yne** might suggest the presence of core-level shifts, caused by an incomplete screening of the core-hole typical for nanostructured gold on poorly conducting substrates, such as SiO<sub>2</sub>.<sup>57</sup>

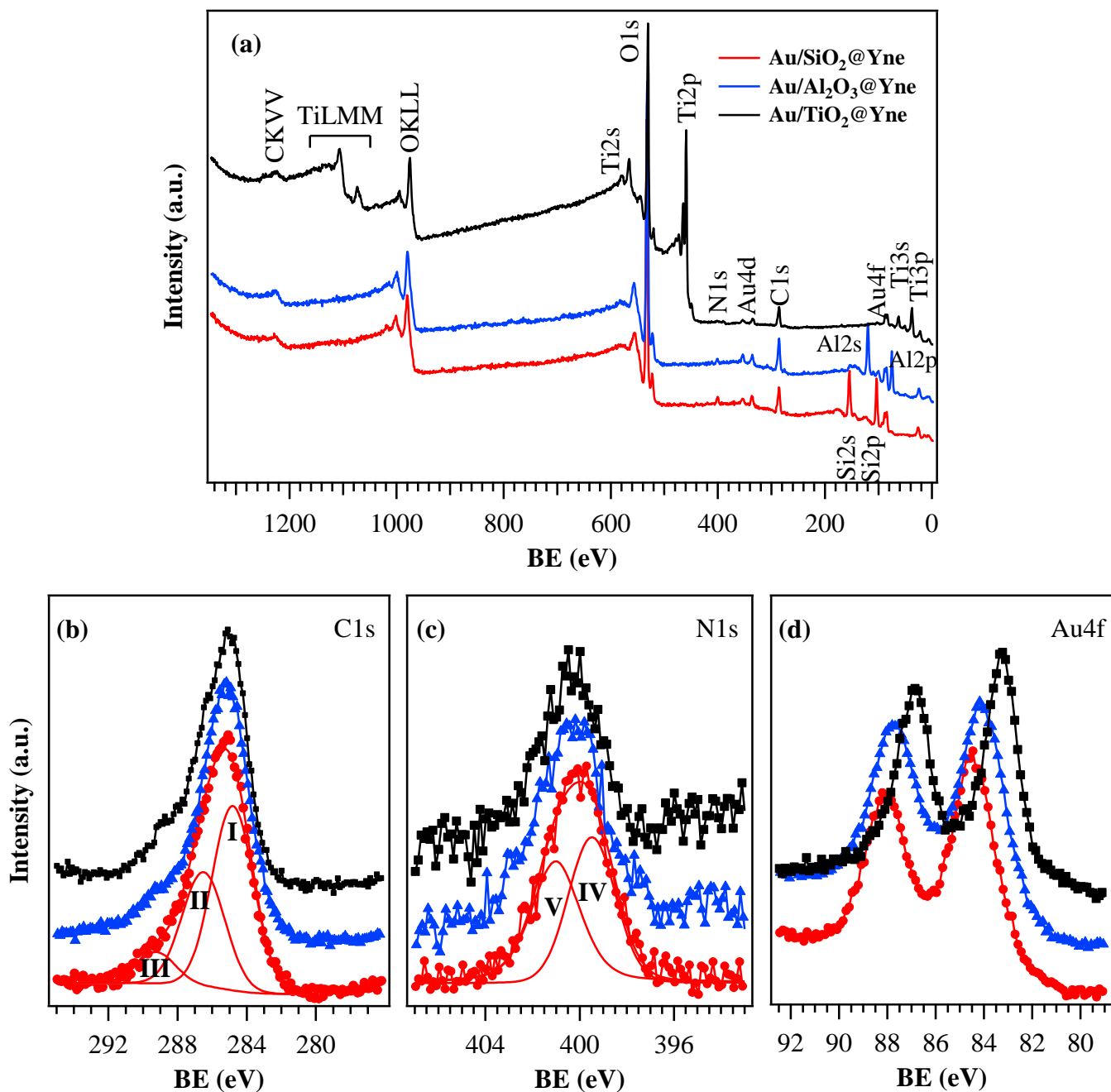


**Figure 3.** Surface wide-scan XP spectra (a) and representative C1s (b), N1s (c) and Au4f (d) photoelectron peaks for the as-prepared specimens.

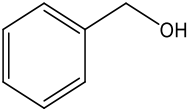
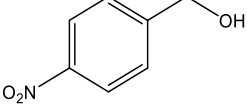
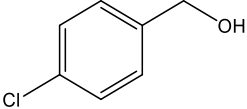
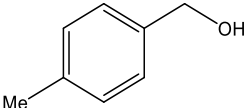
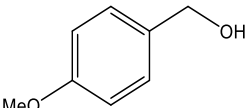
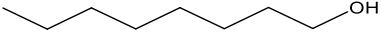
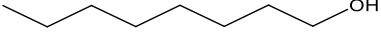
**Catalytic activity of Au/OS@Yne in alcohol oxidation.** The catalytic activity of Au/SiO<sub>2</sub>@Yne was initially studied in the oxidation of a series of benzylic alcohols in a batch system, employing H<sub>2</sub>O<sub>2</sub> as oxidizing agent and water as the reaction medium (Table 2). Under these conditions the

main product of the oxidation reaction was the corresponding carboxylic acid, while the formation of the aldehyde was observed to a lesser extent.

As shown in Table 2 (entry 1), oxidation of benzyl alcohol occurred with a 74% selectivity in benzoic acid and a 26% selectivity in benzaldehyde. The presence of substituents on the aromatic ring was found to affect the alcohol reactivity (Table 2, entries 2-5): the alcohols bearing electron-donating groups (OMe and Me) were completely oxidized in 3 h, whereas 4-chlorobenzyl alcohol was found to be less reactive and in the case of 4-nitrobenzyl alcohol no conversion was observed.

A low conversion was also observed with aliphatic alcohols such as 1-octanol (Table 2, entry 6). In order to attain a comparison with literature data, we also performed the oxidation of 1-octanol with the commercial available AUROLite™ gold catalyst (Au/Mintek) presenting a gold loading of 1 wt%. Before testing, AUROLite was simply ground and sieved to obtain a powder with a granulometry between 60 and 80 mesh, without any further thermal treatment.<sup>14</sup> As shown in Table 2, entry 7, in our hands with this catalyst we obtained a 16% conversion after 1 h, thus confirming the lower activity of this kind of substrates.

**Table 2.** Oxidation of primary alcohols with **Au/SiO<sub>2</sub>@Yne** under batch conditions<sup>a</sup>

Entry	Substrate	t (h)	Conversion (%) <sup>b</sup>	Φ acid (%) <sup>b</sup>	Φ aldehyde (%) <sup>b</sup>
1 <sup>c</sup>		3	86 (84)	74 (70)	26 (30)
2		3	0	-	-
3		5	18	67	33
4		3	>99	>99	-
5		3	>99	61	39
6 <sup>d</sup>		5	30	>99	-
7 <sup>e</sup>		1	16	>99	-

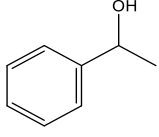
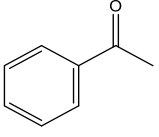
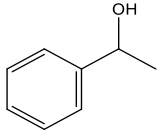
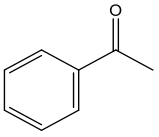
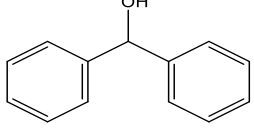
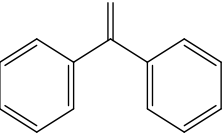
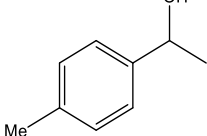
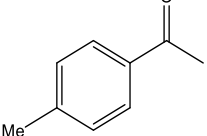
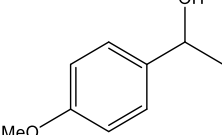
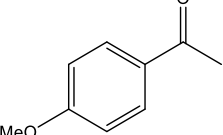
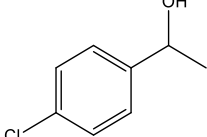
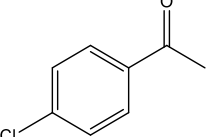
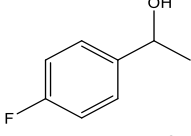
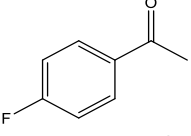
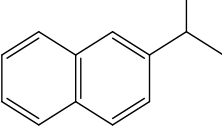
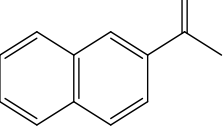
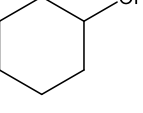
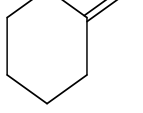
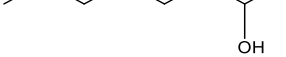
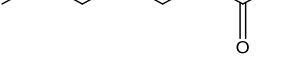
<sup>a</sup>Reaction conditions: starting alcohol solution 0.05 M, solvent: H<sub>2</sub>O, 2.5 mol equiv. H<sub>2</sub>O<sub>2</sub>, T = 90 °C; <sup>b</sup>conversion and selectivity determined by <sup>1</sup>H-NMR; <sup>c</sup>data in parenthesis referred to GC analysis; <sup>d</sup>starting alcohol solution 0.1 M; <sup>e</sup>reaction performed with the catalyst AUROLite™, with a 1.0 M alcohol solution and vertical agitation FirstMate™ synthesizer, Argonaut Technology.

This study was then extended to secondary alcohols though using the solvent system H<sub>2</sub>O/<sup>t</sup>BuOH (6:4 v/v). The use of this solvent mixture instead of just water was dictated by the low solubility in water of some secondary alcohols such as diphenylmethanol as well as the carbonyl products. This problem is mostly stringent when working under continuous-flow conditions (*vide infra*) where the presence of insoluble material must be avoided. The use of water-alcohol mixtures is greener than the use of other common organic solvents;<sup>58</sup> furthermore <sup>t</sup>BuOH has been classified by the Food and Drug Administration as a class 3 solvent.<sup>59</sup>

The results of the experiments, summarized in Table 3, indicated that **Au/SiO<sub>2</sub>@Yne** efficiently catalyzed oxidation of 1-phenylethanol and diphenylmethanol (Table 3, entries 1 and 5).<sup>60</sup> The oxidation of 1-phenylethanol was also performed at a lower temperature (Table 3, entry 4)

leading to a lower conversion value. Therefore, we performed all the subsequent reactions at the temperature of 90 °C. In keeping with what observed with the primary alcohols, the presence of substituents influenced the alcohol reactivity: 1-(p-tolyl)ethanol and 1-(4-methoxyphenyl)ethanol were successfully oxidized in only 1 h (Table 3, entries 6 and 7), while 1-(4-chlorophenyl)ethanol and 1-(4-fluorophenyl)ethanol were found to be less reactive, although a high conversion could still be obtained by increasing the amount of oxidizing agent (Table 3, entries 8 and 9). The catalytic activity of **Au/SiO<sub>2</sub>@Yne** was also tested in the oxidation of an alicyclic and an aliphatic alcohol, i.e. cyclohexanol and 2-octanol, using only water as the reaction medium: however, a lower activity was observed with both substrates (Table 3, entries 11 and 12).

**Table 3.** Oxidation of secondary alcohols with **Au/SiO<sub>2</sub>@Yne** under batch conditions.<sup>a</sup>

Entry	Substrate	Product	t (h)	Conversion (%) <sup>b</sup>
1			4.50	74
2	reuse 1 <sup>c</sup>		4.50	69
3	reuse 2 <sup>c</sup>		4.50	73
4 <sup>d</sup>			4.50	47
5			2	>99
6			1	>99
7			1	>99
8 <sup>e</sup>			6	82
9 <sup>e</sup>			6	55
10			3	90
11 <sup>f,g</sup>			5	46
12 <sup>f</sup>			5	12

<sup>a</sup>Reactions conditions: starting alcohol solution 0.1 M, solvent: H<sub>2</sub>O/<sup>t</sup>BuOH 6:4 v/v, 2.5 mol equiv. H<sub>2</sub>O<sub>2</sub>, 1 % mol Au, T = 90 °C; <sup>b</sup>conversion determined by <sup>1</sup>H-NMR; <sup>c</sup>the catalyst was washed three times with EtOAc before reuse;

<sup>d</sup>reaction performed at T = 70 °C; <sup>e</sup>additional 2.5 mol equiv. of H<sub>2</sub>O<sub>2</sub> were added after 5 h; <sup>f</sup>reaction performed in water; <sup>g</sup>additional 2.5 mol equiv. of H<sub>2</sub>O<sub>2</sub> were added after 2 h.

Recycling experiments were also performed in the oxidation of 1-phenylethanol. After a reaction run the catalyst was recovered by centrifugation, thoroughly washed first with water and then with DCM, dried under vacuum, and reused. With this procedure a decrease of about 50% in the conversion took place already in the second cycle. Conversely, when the catalyst was washed with EtOAc before being reused, the conversion remained essentially the same even after three cycles of reaction (Table 3, entries 2 and 3).<sup>33</sup> The AAS analysis on the recycled catalyst showed that the gold loading after three cycles of reaction was the same of the fresh one. Furthermore, TEM analysis on the reused catalyst indicated that the nanoparticles size distribution remained almost unchanged, though a few larger aggregates were found (Figure S8).

XPS analyses on a representative SiO<sub>2</sub>-supported catalyst after use (Figure S4) yielded analytical data almost identical with respect to the pristine **Au/SiO<sub>2</sub>@Yne** sample, with no significant variations in the relative weight of the different species contributing to C1s and N1s photopeaks. Indeed, the presence of the starting alcohol and the corresponding acid as oxidation product could not be completely ruled out, since they would give rise to signals completely overlapped with components **I** and **II** in the C1s signal, and indistinguishable from the main O1s photopeak. Taken together, these results enabled to rule out the occurrence of significant chemical changes in the nature and chemical state of the observed species.

Subsequently, basing on the above results, we chose to perform the oxidation of alcohols catalyzed by **Au/SiO<sub>2</sub>@Yne** in a continuous flow system (Table 4). The flow reactor was packed with the catalyst, heated to 90 °C and fed with the reagent mixture at the constant flow rate of 0.1 mL min<sup>-1</sup>.<sup>61</sup> Under these conditions, 1-phenylethanol was converted to acetophenone with a 85 % yield, with the system achieving the steady-state regime after 2 h (Table 4, entry 1).

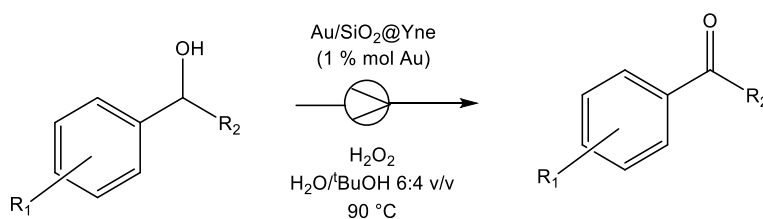
In order to enhance the conversion of the substrate, a catalytic test at a lower flow rate was also performed (Table 4, entry 2); however no significant differences were observed.

The long-term stability of **Au/SiO<sub>2</sub>@Yne** was also investigated and it was found that the catalyst could work for over 50 h without observing any significant decreasing in the catalytic activity.

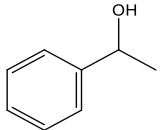
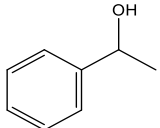
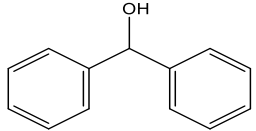
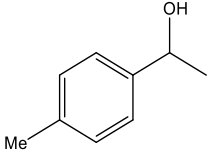
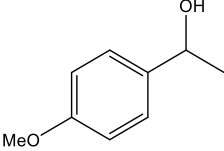
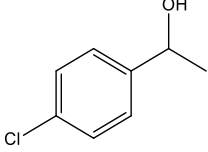
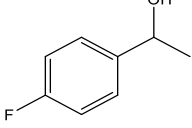
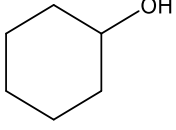
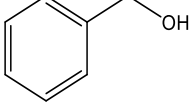
The improvement in the catalyst performances under these conditions was particularly evident in the oxidation of the less reactive substrates. Indeed, in the case 1-(4-chlorophenyl)ethanol and 1-(4-fluorophenyl)ethanol the conversions achieved in the flow system after 1 h (Table 4, entries 6-7) were comparable to those achieved in the batch system in 6 h (Table 3, entries 8 and 9).

Moreover, the oxidation of benzyl alcohol was successfully carried out in the continuous-flow system (Table 4, entry 9), giving an almost complete conversion with a 100 % selectivity in the corresponding carboxylic acid.

**Table 4.** Oxidation of alcohols with **Au/SiO<sub>2</sub>@Yne** in continuous-flow system.<sup>a</sup>





Entry	Substrate	t (h) <sup>b</sup>	Conversion (%) <sup>c</sup>
1		2	85
2 <sup>d</sup>		2	90
3		3	96
4		1	>99
5		1	>99
6		1	77
7 <sup>e</sup>		1	68
8 <sup>f</sup>		2	15
9 <sup>g</sup>		2	>99 <sup>h</sup>

<sup>a</sup>Reactions conditions: starting alcohol solution 0.1 M, solvent: H<sub>2</sub>O/<sup>t</sup>BuOH 6:4, 2.5 mol equiv. H<sub>2</sub>O<sub>2</sub>, T<sub>solution</sub> = 30 °C, T<sub>reactor</sub> = 90 °C; flow rate: 0.1 mL min<sup>-1</sup>; <sup>b</sup>time needed to achieve the steady-state regime; <sup>c</sup>steady-state conversion determined by <sup>1</sup>H-NMR; <sup>d</sup>reaction performed at a flow rate of 0.075 mL min<sup>-1</sup>; <sup>e</sup>the reaction was performed at 80 °C, <sup>f</sup>reaction performed in water, with 5 equivalents of H<sub>2</sub>O<sub>2</sub>, at a flow rate of 0.05 mL min<sup>-1</sup>; <sup>g</sup>reaction performed in water at a flow rate of 0.3 mL min<sup>-1</sup> with a starting alcohol concentration of 0.025 M; <sup>h</sup>complete selectivity in the corresponding carboxylic acid.

The catalytic activity of **Au/Al<sub>2</sub>O<sub>3</sub>@Yne** and **Au/TiO<sub>2</sub>@Yne** in the oxidation of 1-phenylethanol in batch and flow conditions was also evaluated and compared to the catalytic activity of the silica-supported catalyst (Table 5). In batch experiments **Au/SiO<sub>2</sub>@Yne** was found to be the most active of the tested catalysts, leading to a 74% conversion of the substrate after 4.50 h (entry 1 of Tables 4 and 5), while with **Au/Al<sub>2</sub>O<sub>3</sub>@Yne** a final conversion of only 28% was achieved in the same amount of time (Table 5, entry 2). The titania-supported catalyst showed almost no catalytic activity in the target reaction (Table 5, entry 3). These results could be explained by the different Au<sub>NPs</sub> size dimension and distribution of the three catalysts.<sup>14,62-65</sup> However, in the case of **Au/TiO<sub>2</sub>@Yne**, the very low conversion was mainly due to the fact that, under batch conditions, the starting size (60 ÷ 80 mesh) of the support was completely lost: this gives a very fine powder, difficult to separate from the supernatant at the end of the reaction, where all Au<sub>NPs</sub> are probably not exposed any longer on the catalyst surface. Indeed, no significant improvements were observed by carrying out the reaction with the FirstMate<sup>TM</sup> synthesizer that provides a milder vertical agitation. On the other hand, when the reaction was performed in the flow system, significant improvements were observed. Upon using the **Au/Al<sub>2</sub>O<sub>3</sub>@Yne** catalyst, the conversion increased from 28% to 85% (Table 5, entry 2), hence becoming comparable to **Au/SiO<sub>2</sub>@Yne**, whilst for **Au/TiO<sub>2</sub>@Yne** a dramatic increase from 2 % to 80% occurred (Table 5, entry 3).<sup>66</sup>

**Table 5.** Oxidation of 1-phenylethanol with the synthesized catalysts in batch<sup>a</sup> and flow.<sup>b</sup>

Entry	Catalyst	BATCH		FLOW
		Conversion (%) <sup>c</sup>	Conversion (%) <sup>c</sup>	Productivity (h <sup>-1</sup> ) <sup>d</sup>
1	<b>Au/SiO<sub>2</sub>@Yne</b>	74	85	12.8
2	<b>Au/Al<sub>2</sub>O<sub>3</sub>@Yne</b>	28	85	10.2
3	<b>Au/TiO<sub>2</sub>@Yne</b>	2 <sup>e</sup>	80 <sup>f</sup>	19.2

<sup>a</sup>Reactions conditions: starting alcohol solution 0.1 M, solvent: H<sub>2</sub>O/<sup>t</sup>BuOH 6:4 v/v, 2.5 mol equiv. H<sub>2</sub>O<sub>2</sub>, 1 % mol Au, T = 90°C, 4.50 h; <sup>b</sup>reactions conditions: starting alcohol solution 0.1 M, solvent: H<sub>2</sub>O/<sup>t</sup>BuOH 6:4 v/v, 2.5 mol equiv. H<sub>2</sub>O<sub>2</sub>, T<sub>solution</sub> = 30 °C, T<sub>reactor</sub> = 90 °C; flow rate: 0.1 mL min<sup>-1</sup>, steady-state achieved after 2 h; <sup>c</sup>conversion

determined by  $^1\text{H-NMR}$ ; <sup>d</sup>calculated as mole of product per mole of Au per time. <sup>e</sup>vertical agitation was performed with the FirstMate™ synthesizer, Argonaut Technology; <sup>f</sup> steady-state achieved after 4 h.

These results clearly demonstrate that for our systems the flow approach also plays a strategic role in preserving the physical and chemical integrity of the solid catalyst during its use.

## Conclusions

This paper reports the synthesis of systems based on *in-situ* formed Au<sub>NPs</sub> tethered on alkynyl carbamate-modified commercial, micrometer-sized silica, aluminium oxide and titanium oxide (**Au/SiO<sub>2</sub>@Yne**, **Au/Al<sub>2</sub>O<sub>3</sub>@Yne**, **Au/TiO<sub>2</sub>@Yne**) suitable for being employed as catalysts in the oxidation of alcohols in continuous-flow packed bed reactors.

From a comparison between the results obtained from the three catalytic systems the following conclusions can be drawn.

Silica allowed the highest organic functionalization (12 wt%) as well as the highest gold loading (3.7 wt%). Moreover, TEM microscopy investigation showed only for **Au/SiO<sub>2</sub>@Yne** the presence of homogeneously distributed, spherically shaped Au<sub>NPs</sub> (av. diameter 15 nm). XPS analyses carried out on the three different specimens revealed that their surfaces were decorated with pure Au nanoparticles, and no signals related to Au(I) and Au(III) species could be identified.

**Au/SiO<sub>2</sub>@Yne** efficiently catalyzed, both in batch and flow conditions, the oxidation of a large variety of alcohols. Furthermore, under flow conditions, the catalyst could work for over 50 h at 90 °C without observing any significant decrease in the catalytic activity.

A comparison among the catalytic activities of **Au/SiO<sub>2</sub>@Yne**, **Au/Al<sub>2</sub>O<sub>3</sub>@Yne**, and **Au/TiO<sub>2</sub>@Yne** in the oxidation of 1-phenylethanol, carried out both in batch and in continuous-flow system, demonstrated that, although **Au/SiO<sub>2</sub>@Yne** gave the best overall performances, the flow methodology plays a strategic role in preserving the physical and chemical integrity of the

solid catalyst during its use, with dramatic consequences, in the case of **Au/TiO<sub>2</sub>@Yne**, as far as the reaction conversion is concerned (from 2% in batch to 80 % in flow).

XPS analyses suggested the occurrence of different charge levels at the gold particles depending on the substrate and this could be in principle related to the observed different activities of the three catalysts. Nevertheless, as far as a full rationalization of the experimental results is concerned, this point cannot be conclusive, since a complete rationale of the role of gold in such mechanisms has not been attained yet.<sup>63,67</sup>

Finally, it is worth pointing out that our systems are extremely straightforward to be obtained, with a high reproducibility as well, starting from commercially available supports. They can be recycled in batch conditions with almost no loss of activity and they are suitable, robust materials for working under continuous-flow conditions.

### **Supporting Information**

Instruments and methods; additional spectroscopic and analytical data (AAS, TGA, TEM, XPS, ATR-FTIR, GC) for **Au/OS@Yne**; catalysis additional information (<sup>1</sup>H-NMR spectrum of the oxidation of 1-phenylethanol, continuous-flow set-up scheme). The material is available free of charge via the Internet at <http://pubs.acs.org>

### **Acknowledgments**

The authors wish to thank the University of Bologna for financial support. D. N. acknowledges support by a grant from the Italian MIUR (PRIN 2010-2011-010PFLRJR, “PROxi” project). The authors also gratefully thank Dr. Stefano Cerini and Alberto Mucchi for AAS measurements, Dr. Katia Rubini for TGA analysis, and Flavien Garcia Moran (Chimie ParisTech) for experimental support.

## References and Notes

- (1) Sheldon, R. A. Fundamentals of green chemistry: efficiency in reaction design. *Chem. Soc. Rev.* **2012**, *41*, 1437-1451.
- (2) Sheldon, R. A. *Metal-Catalyzed Reactions in Water*; Wiley-VCH Verlag GmbH & Co. KGaA: Weinheim, Germany, 2013.
- (3) Sheldon, R. A.; Arends, I. W. C. E.; Ten Brink, G.-J.; Dijkstra, A. Green, catalytic oxidations of alcohols. *Acc. Chem. Res.* **2002**, *35*, 774-781.
- (4) Pagliaro, M.; Campestrini, S.; Ciriminna, R. Ru-based oxidation catalysis. *Chem. Soc. Rev.* **2005**, *34*, 837-845.
- (5) Philippot, K.; Serp, P. Eds. *Nanomaterials in Catalysis*; Wiley-VCH: Weinheim, Germany, 2013.
- (6) Corma, A.; Garcia, H. Supported gold nanoparticles as catalysts for organic reactions. *Chem. Soc. Rev.* **2008**, *37*, 2096-2126.
- (7) Della Pina, C.; Falletta, E.; Prati, L.; Rossi, M. Selective oxidation using gold. *Chem. Soc. Rev.* **2008**, *37*, 2077-2095.
- (8) Della Pina, C.; Falletta, E.; Rossi, M. Update on selective oxidation using gold. *Chem. Soc. Rev.* **2012**, *41*, 350-369.
- (9) Zhang, Y.; Cui, X.; Shi, F.; Deng, Y. Nano-gold catalysis in fine chemical synthesis. *Chem. Rev.* **2012**, *112*, 2467-2505.
- (10) Davis, S. E.; Ide, M. S.; Davis, R. J. Selective oxidation of alcohols and aldehydes over supported metal nanoparticles. *Green Chem.* **2013**, *15*, 17-45.
- (11) Enache, D. I.; Knight, D. W.; Hutchings, G. J. Solvent-free oxidation of primary alcohols to aldehydes using supported gold catalysts. *Catal. Lett.* **2005**, *103*, 43-52.
- (12) Hu, J.; Chen, L.; Zhu, K.; Suchopar, A.; Richards, R. Aerobic oxidation of alcohols catalyzed by gold nano-particles confined in the walls of mesoporous silica. *Catal. Today* **2007**, *122*, 277-283.

- (13) Kim, S.; Bae, S. W.; Lee, J. S.; Park, J. Recyclable gold nanoparticle catalyst for the aerobic alcohol oxidation and C–C bond forming reaction between primary alcohols and ketones under ambient conditions. *Tetrahedron* **2009**, *65*, 1461-1466.
- (14) Ni, J.; Yu, W.-J.; He, L.; Sun, H.; Cao, Y.; He, H.-Y.; Fan, K.-N. A green and efficient oxidation of alcohols by supported gold catalysts using aqueous H<sub>2</sub>O<sub>2</sub> under organic solvent-free conditions. *Green Chem.* **2009**, *11*, 756-759.
- (15) Ma, C. Y.; Cheng, J.; Wang, H. L.; Hu, Q.; Tian, H.; He, C.; Hao, Z. P. Characteristics of Au/HMS catalysts for selective oxidation of benzyl alcohol to benzaldehyde. *Catal. Today* **2010**, *158*, 246-251.
- (16) Li, H.; Zheng, Z.; Cao, M.; Cao, R. Stable gold nanoparticle encapsulated in silica-dendrimers organic–inorganic hybrid composite as recyclable catalyst for oxidation of alcohol. *Micropor. Mesopor. Mat.* **2010**, *136*, 42-49.
- (17) Wang, L.; Yi, W.; Cai, C. A green and highly selective oxidation of alcohols by fluorosilica gel-supported gold nanoparticles in aqueous H<sub>2</sub>O<sub>2</sub> under base-free conditions. *ChemSusChem*, **2010**, *3*, 1280-1284.
- (18) Shang, C.; Liu, Z.-P. Origin and activity of gold nanoparticles as aerobic oxidation catalysts in aqueous solution. *J. Am. Chem. Soc.* **2011**, *133*, 9938-9947.
- (19) Asao, N.; Hatakeyama, N.; Menggenbateer; Minato, T.; Ito, E.; Hara, M.; Kim, Y.; Yamamoto, Y.; Chen, M.; Zhang, W.; Inoue, A. Aerobic oxidation of alcohols in the liquid phase with nanoporous gold catalysts. *Chem. Commun.* **2012**, *48*, 4540-4542.
- (20) Ftouni, J.; Penhoat, M.; Girardon, J.-S.; Addad, A.; Payen, E.; Rolando, C. Immobilization of gold nanoparticles on fused silica capillary surface for the development of catalytic microreactors. *Chem. Eng. J.* **2013**, *227*, 103-110.
- (21) Rautiainen, S.; Simakova, O.; Guo, H.; Leino, A.-R.; Kordás, K.; Murzin, D.; Leskelä, M.; Repo, T. Solvent controlled catalysis: Synthesis of aldehyde, acid or ester by selective oxidation of benzyl alcohol with gold nanoparticles on alumina. *Appl. Catal. A*, **2014**, *485*, 202-206.

- (22) Ciriminna, R.; Fidalgo, A.; Pandarus, V.; Béland, F.; Ilharco, L. M.; Pagliaro, M. New catalyst series from the sol–gel-entrapment of gold nanoparticles in organically modified silica matrices: proof of performance in a model oxidation reaction. *ChemCatChem* **2015**, *7*, 254-260.
- (23) Sharma, A. S.; Kaur, H.; Shah, D. Selective oxidation of alcohols by supported gold nanoparticles: recent advances. *RSC Adv.* **2016**, *6*, 28688-28727.
- (24) Wiles, C.; Watts, P. Continuous flow reactors: a perspective. *Green Chem.* **2012**, *14*, 38-54.
- (25) Wiles, C.; Watts, P. Continuous process technology: a tool for sustainable production. *Green Chem.*, **2014**, *16*, 55-62.
- (26) Gutmann, B.; Cantillo, D.; Kappe, C. O. Continuous-flow technology—a tool for the safe manufacturing of active pharmaceutical ingredients. *Angew. Chem. Int. Ed.*, **2015**, *54*, 6688-6728.
- (27) Wegner, J.; Ceylan, S.; Kirschning, A. Ten key issues in modern flow chemistry. *Chem. Comm.* **2011**, *47*, 4593-4592.
- (28) Ricciardi, R.; Huskens, J.; Verboom, W. Nanocatalysis in flow. *ChemSusChem* **2015**, *8*, 2586-2605.
- (29) Gemoets, H. P. L.; Su, Y.; Shang, M.; Hessel, V.; Luque, R.; Noël, T. Liquid phase oxidation chemistry in continuous flow microreactors. *Chem. Soc. Rev.* **2016**, *45*, 83-117.
- (30) Dambruoso, P.; Ballestri, M.; Ferroni, C.; Guerrini, A.; Sotgiu, G.; Varchi, G.; Massi, A. TPPS supported on core–shell PMMA nanoparticles: the development of continuous flow membrane-mediated electrocoagulation as a photocatalyst processing method in aqueous media. *Green Chem.* **2015**, *17*, 1907-1917.
- (31) Fazzini, S.; Nanni, D.; Ballarin, B.; Cassani, M. C.; Giorgetti, M.; Maccato, C.; Trapananti, A.; Aquilanti, G.; Ahmed, S. I. Straightforward synthesis of gold nanoparticles supported on commercial silica-polyethyleneimine beads. *J. Phys. Chem. C* **2012**, *116*, 25434-25443.
- (32) Fazzini, S.; Cassani, M. C.; Ballarin, B.; Boanini, E.; Girardon, J.-S.; Mamede, A.-S.; Mignani, A.; Nanni, D. Novel synthesis of gold nanoparticles supported on alkyne-functionalized nanosilica. *J. Phys. Chem. C* **2014**, *118*, 24538-24547.

- (33) Giorgetti, M.; Aquilanti, G.; Ballarin, B.; Berrettoni, M.; Cassani, M. C.; Fazzini, S.; Nanni, D.; Tonelli, D. Speciation of gold nanoparticles by ex situ extended X-ray absorption fine structure and X-ray absorption near edge structure. *Anal. Chem.*, **2016**, *88*, 6873-6880.
- (34) Cassani, M. C.; Ballarin, B.; Barreca, D.; Boanini, E.; Bonansegna, E.; Carraro, G.; Fazzini, S.; Mignani, A.; Nanni, D.; Pinelli, D. Functionalization of silica through thiol-yne radical chemistry: a catalytic system based on gold nanoparticles supported on amino-sulfidebranched silica. *RSC Adv.* **2016**, *6*, 25780-25788.
- (35) Ma, Z.; Dai, S. *Heterogeneous Gold Catalysts and Catalysis*; The Royal Society of Chemistry, 2014, RSC Catalysis Series N°. 18, 1.
- (36) Schauermaun, S.; Nilius, N.; Shaikhutdinov, S.; Freund, H.-J. Nanoparticles for heterogeneous catalysis: new mechanistic insights. *Acc. Chem. Res.* **2013**, *46*, 1673-1681.
- (37) Braurer, G. *Handbook of Preparative Inorganic Chemistry*; Academic Press: New York, 1963, Vol. II, 1058.
- (38) Perrin, D. D.; Armarego, W. L. F.; Perrin, D. R. *Purification of Laboratory Chemicals*; Pergamon Press: New York, 2<sup>nd</sup> edn, 1980.
- (39) Briggs, D.; Seah, M. P.; *Practical Surface Analysis by Auger and X-ray Photoelectron Spectroscopy*; Wiley: New York, 2<sup>nd</sup> edn. 1990.
- (40) Moulder, J. F.; Stickle, W. F.; Sobol, P. E.; Bomben, K. D.; *Handbook of X-ray Photoelectron Spectroscopy*; Perkin Elmer Corporation: Eden Prairie, MN, 1992.
- (41) Shirley, D. High-resolution X-ray photoemission spectrum of the valence bands of gold. *Phys. Rev. B* **1972**, *5*, 4709-47013.
- (42) In order to avoid mechanical stirring, the preparation of **Au/TiO<sub>2</sub>@Yne** was performed in a rotary evaporator.
- (43) The presence of the organic functionalization was found to be essential for the deposition of gold nanoparticles on the support, since when a H<sub>2</sub>AuCl<sub>4</sub> solution was added to a suspension of bare support no reduction/immobilization of gold was observed.

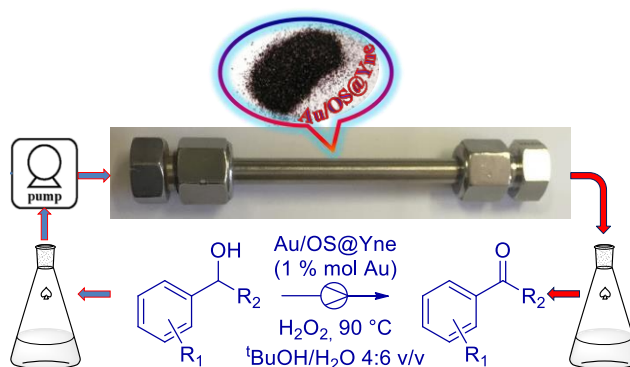


- (44) Furer, K. L. Hydrogen bonding in ethyl carbamate studied by IR spectroscopy. *J. Mol. Struct.* **1998**, *449*, 53-59.
- (45) The preparation of **Au/SiO<sub>2</sub>@Yne** containing a 13 wt% of gold was carried out as follows. In a 250 mL three-necked dry round-bottomed flask under a N<sub>2</sub> atmosphere, a suspension of 0.370 g of **SiO<sub>2</sub>@Yne** and 90 mL of H<sub>2</sub>O was heated to 90 °C. When the system had reached the desired temperature, 90 mL of a 3.0 mM solution of H<sub>2</sub>AuCl<sub>4</sub> was rapidly added and the reaction mixture was left under stirring for 1 h. At the end of the reaction the obtained dark purple solid material was separated from the supernatant solution by centrifugation (5600 rpm, 15 min) and re-dispersed twice in water and twice in EtOH, then it was dried under a nitrogen flow and the Au content was determined by AAS spectroscopy before SS NMR analysis.
- (46) Blümel, J. Reactions of ethoxysilane with silica: a solid-state nmr study. *J. Am. Chem. Soc.* **1995**, *117*, 2112-2113.
- (47) Zhang, L. Tandem Au-catalyzed 3,3-rearrangement-[2 + 2] cycloadditions of propargylic esters: expeditious access to highly functionalized 2,3-indoline-fused cyclobutanes. *J. Am. Chem. Soc.* **2005**, *127*, 16804–16805.
- (48) Li, G.; Zhang, G.; Zhang, L. Au-catalyzed synthesis of (1Z, 3E)-2-pivaloxy-1,3-dienes from propargylic pivalates. *J. Am. Chem. Soc.* **2008**, *130*, 3740–3741.
- (49) Shi, F.-Q.; Li, X.; Xia, Y.; Zhang, L.; Yu, Z.-X. A DFT study of the mechanisms of “in water” Au(I)-catalyzed tandem [3,3] rearrangement/nazarov reaction/[1,2]-hydrogen shift of enynyl acetates: a proton-transport catalysis strategy in the water-catalyzed [1,2]-hydrogen shift. *J. Am. Chem. Soc.* **2007**, *129*, 15503–15512.
- (50) Sui, R.; Lesage, K. L.; Carefoot, S. K.; Fürstehaupt, T.; Rose, C. J.; Marriott, R. A. Selective adsorption of thiols using gold nanoparticles supported on metal oxides. *Langmuir* **2016**, *32*, 9197-9205.
- (51) Filonenko, G. A.; Vrijburg, W. L.; Hensen, E. J. M.; Pidko, E. A. On the activity of supported Au catalysts in the liquid phase hydrogenation of CO<sub>2</sub> to formates, *J. Catal.* **2016**, *343*, 97-105.

- (52) Li, M.; Wang, X.; Cárdenas-Lizana, F.; Keane, M. A. Effect of support redox character on catalytic performance in the gas phase hydrogenation of benzaldehyde and nitrobenzene over supported gold. *Catal. Today* **2017**, *279*, 19-28.
- (53) Panthi, B.; Mukhopadhyay, A.; Tibbitts, L.; Saavedra, J.; Pursell, C. J.; Rioux, R. M.; Chandler, B. D. Using thiol adsorption on supported Au nanoparticle catalysts to evaluate Au dispersion and the number of active sites for benzyl alcohol oxidation. *ACS Catal.* **2015**, *5*, 2232-2241.
- (54) Perret, N.; Wang, X.; Onfroy, T.; Calers, C.; Keane, M. A. Selectivity in the gas-phase hydrogenation of 4-nitrobenzaldehyde over supported Au catalysts. *J. Catal.* **2014**, *309*, 333-342.
- (55) Zhao, C.; Li, B.; Du, J.; Chen, J.; Li, Y. Microstructure and optical absorption property of Au nanoparticles and Au, Ag bimetal nanoparticles separately dispersed Al<sub>2</sub>O<sub>3</sub> composite films. *J. Alloy Compd.* **2017**, *691*, 772-777.
- (56) Perret, N.; Wang, X.; Onfroy, T.; Calers, C.; Keane, M. A. Selectivity in the gas-phase hydrogenation of 4-nitrobenzaldehyde over supported Au catalysts. *J. Catal.* **2014**, *309*, 333-342.
- (57) Barreca, D.; Bovo, A.; Gasparotto, A.; Tondello, E. Au/SiO<sub>2</sub> nanosystems by XPS. *Surf. Sci. Spectra* **2003**, *10*, 21-31.
- (58) Capello, C.; Fischer, U.; Hungerbühler, K. Nanoparticles for heterogeneous catalysis: new mechanistic insights. *Green Chem.* **2007**, *9*, 927-934.
- (59) U.S. Food and Drug Administration, <http://www.fda.gov/default.htm>
- (60) Additionally, two blank reactions were carried out, one in absence of the catalyst and one in absence of the oxidizing agent H<sub>2</sub>O<sub>2</sub>, but no conversion of the alcohol was observed indicating that both **Au/SiO<sub>2</sub>@Yne** and hydrogen peroxide are needed for the reaction to take place.
- (61) The residence time of our flow system is 2.5 min at 0.1 mL min<sup>-1</sup> as determined by pycnometric measurements. If compared to the reaction time of the batch experiments (1-4 h), this data further confirmed the significant improvement of catalyst activity moving from batch to flow conditions.

- (62) Haruta, M. Size- and support-dependency in the catalysis of gold. *Catal. Today* **1997**, *36*, 153-166.
- (63) Abad, A.; Corma, A.; Garcia, H. Catalyst parameters determining activity and selectivity of supported gold nanoparticles for the aerobic oxidation of alcohols: the molecular reaction mechanism. *Chem. Eur. J.* **2008**, *14*, 212-222.
- (64) Comotti, M.; Della Pina, C.; Matarrese, R.; Rossi, M. The catalytic activity of “naked” gold particles. *Angew. Chem., Int. Ed.* **2004**, *43*, 5812-5815.
- (65) Panigrahi, S.; Basu, S.; Praharaj, S.; Pande, S.; Jana, S.; Pal, A.; Ghosh, S. K.; Pal, T. Synthesis and size-selective catalysis by supported gold nanoparticles: study on heterogeneous and homogeneous catalytic process. *J. Phys. Chem. C* **2007**, *111*, 4596-4605.
- (66) Various blank reactions were carried out under flow conditions with the reactor packed with **SiO<sub>2</sub>**, **SiO<sub>2</sub>@Yne**, **Al<sub>2</sub>O<sub>3</sub>**, **Al<sub>2</sub>O<sub>3</sub>@Yne**, **TiO<sub>2</sub>**, and **TiO<sub>2</sub>@Yne**, but no conversion of the alcohol was observed in any case.
- (67) Conte, M.; Miyamura, H.; Kobayashi, S.; Chechik, V. Spin trapping of Au-H intermediate in the alcohol oxidation by supported and unsupported gold catalysts. *J. Am. Chem. Soc.* **2009**, *131*, 7189-7196.

## For Table of Contents Use Only



## Synopsis

$\text{Au}_{\text{NPs}}$  were straightforwardly anchored on alkynyl carbamate-functionalized commercial supports (silica, alumina, and titania) for application as alcohol oxidation catalysts in continuous-flow packed bed reactors.